THE JOURNAL OF BIOLOGICAL CHEMISTRY VOL. 287, NO. 49, pp. 41245–41257, November 30, 2012

Discovery of AZD3839, a Potent and Selective BACE1 Inhibitor Clinical Candidate for the Treatment of Alzheimer Disease*[S]

Received for publication, August 9, 2012, and in revised form, September 24, 2012 Published, JBC Papers in Press, October 9, 2012, DOI 10.1074/jbc.M112.409110

Fredrik Jeppsson[‡§], Susanna Eketjäll[‡¶], Juliette Janson[‡], Sofia Karlström[‡], Susanne Gustavsson[‡], Lise-Lotte Olsson[‖], Ann-Cathrine Radesäter[‡], Bart Ploeger[‡], Gvido Cebers[**], Karin Kolmodin[‡], Britt-Marie Swahn[‡], Stefan von Berg[‡], Tjerk Bueters[‡], and Johanna Fälting[‡1]

From the [‡]Innovative Medicines AstraZeneca, CNS and Pain, 15185 Södertälje, Sweden, [§]Science for Life Laboratory, Division of Translational Medicine and Chemical Biology, Department of Medical Biochemistry and Biophysics, Karolinska Institutet, 17165 Solna, Sweden, [¶]AstraZeneca Translational Sciences Centre, Science for Life Laboratory, 17165 Solna, Sweden, [‖]Discovery Sciences, AstraZeneca, 43153 Mölndal, Sweden, and [**]AstraZeneca Neuroscience, Cambridge, Massachusetts 02139

Background: BACE1 inhibitors target the first step in Aβ formation and are tractable drugs for halting disease progression in Alzheimer disease.
Results: AZD3839 is a novel BACE1 inhibitor that effectively reduces brain and CSF Aβ levels in several preclinical species.
Conclusion: Based on the preclinical profile, AZD3839 was progressed into Phase I.
Significance: AZD3839 may have disease-modifying potential in the treatment of Alzheimer disease.

β-Site amyloid precursor protein cleaving enzyme1 (BACE1) is one of the key enzymes involved in the processing of the amyloid precursor protein (APP) and formation of amyloid β peptide (Aβ) species. Because cerebral deposition of Aβ species might be critical for the pathogenesis of Alzheimer disease, BACE1 has emerged as a key target for the treatment of this disease. Here, we report the discovery and comprehensive preclinical characterization of AZD3839, a potent and selective inhibitor of human BACE1. AZD3839 was identified using fragment-based screening and structure-based design. In a concentration-dependent manner, AZD3839 inhibited BACE1 activity in a biochemical fluorescence resonance energy transfer (FRET) assay, Aβ and sAPPβ release from modified and wild-type human SH-SY5Y cells and mouse N2A cells as well as from mouse and guinea pig primary cortical neurons. Selectivity against BACE2 and cathepsin D was 14 and >1000-fold, respectively. AZD3839 exhibited dose- and time-dependent lowering of plasma, brain, and cerebrospinal fluid Aβ levels in mouse, guinea pig, and non-human primate. Pharmacokinetic/pharmacodynamic analyses of mouse and guinea pig data showed a good correlation between the potency of AZD3839 in primary cortical neurons and *in vivo* brain effects. These results suggest that AZD3839 effectively reduces the levels of Aβ in brain, CSF, and plasma in several preclinical species. It might, therefore, have disease-modifying potential in the treatment of Alzheimer disease and related dementias. Based on the overall pharmacological profile and its drug like properties, AZD3839 has been progressed into Phase 1 clinical trials in man.

Alzheimer disease (AD)[2] is a progressive neurodegenerative disorder manifested by cognitive and memory deterioration (1). Worldwide, more than 35 million people suffer from AD, and the prevalence is increasing due to an aging population and higher diagnosis rates (2–3). Currently available drug therapies provide only symptomatic treatment and are generally viewed as minimally effective with only minor improvements for a limited duration (4–6). There is a huge unmet medical need for drugs that modify AD pathology, thereby slowing or delaying the onset of disease progression, allowing patients to maintain their independence.

Cleavage of amyloid precursor protein (APP) by β-secretase (β-site amyloid precursor protein cleaving enzyme 1 (BACE1)) and subsequently γ-secretase, gives rise to peptide fragments known as amyloid β peptides (Aβ) (7–13). Increased extracellular accumulation of Aβ, in particular Aβ42, results in the formation of Aβ oligomers, cerebral amyloid plaques, neurodegeneration, and ultimately brain atrophy (14). Amyloid pathology together with neurofibrillary tangles are major hallmarks of pathology in AD (15–16). Changes in production, processing, and/or clearance of brain Aβ levels are believed to be key events in the pathophysiology of both sporadic and early onset AD. Therefore, modulation of Aβ production is considered one of the highest priority drug targets in the AD field (6, 17). BACE1 and γ-secretase also act on other substrates in addition to APP; however, as these substrates may have neurobiological significance, partial reduction of the activity of BACE1 or modulation of the γ-secretase complex may be attractive approaches for disease modification in AD (18).

Increased expression and activity of BACE1 in post-mortem brains of AD patients compared with age-matched controls have been reported (19–20). BACE1 has been shown to be ele-

* This work was supported by AstraZeneca.
[S] This article contains supplemental data.
[1] To whom correspondence should be addressed: AstraZeneca R&D, Innovative Medicines, CNS and Pain, Södertälje, Sweden. Tel.: 46-8-55322617; Fax: 46-8-553 28450; E-mail: Johanna.Falting@astrazeneca.com.

[2] The abbreviations used are: AD, Alzheimer disease; Aβ, amyloid β; APP, amyloid precursor protein; sAPPb, soluble amyloid precursor protein b; BACE, β secretase; CSF, cerebrospinal fluid; PKPD, pharmacokinetic/pharmacodynamic; h-, human.

vated in cerebrospinal fluid (CSF) of prodromal AD patients (21). In addition, disease linkage in man is supported by specific autosomal dominant disease-causing mutations in the APP gene (APP carrying the Swedish mutation (APPswe)) resulting in an increased affinity of APP binding to BACE1 and, consequently, increased Aβ production (11). Recently, discovery of a variant of the APP gene (APPA673T) at a site proximal to the BACE1 proteolytic site that confers protection against AD was reported (22). A673T substitution in APP reduces BACE1 cleavage relative to wild-type APP substrates and thus provides further support for the idea that blocking BACE1 cleavage of APP may protect against AD. Several studies have convincingly demonstrated that reduction of BACE1 activity can alter amyloid burden in mice (23–29). Recently, emerging data showed that BACE1 inhibitors also were able to lower CSF Aβ levels in humans in Phase I clinical studies (30). Although many research groups have been aiming to find small molecule inhibitors of BACE1, the development of such inhibitors has been challenging (31). BACE1 x-ray studies have revealed a wide open active site with a flexible loop and few hot spots for interaction (32). In addition, it has been difficult to modify cerebral Aβ levels in preclinical animal models. Major obstacles have been low oral bioavailability and restricted brain exposure caused by affinity for drug transporter proteins (33–35) resulting in low drug concentrations at the target site. Here, we report the discovery and pharmacological profile of a potent and selective orally active, brain-permeable BACE1 inhibitor AZD3839, a clinical candidate that recently progressed into Phase 1 clinical trials in man.

EXPERIMENTAL PROCEDURES

Protein Crystallography—Protein expression and purification for structural studies was done as previously described by Patel *et al.* (36). Crystallization of compounds bound to BACE1 has been described by Swahn *et al.* (37). Crystallographic data of BACE1 in complex with AZD3839 were collected to 1.8 Å resolution on a Rigaku FR-E generator equipped with a MarMosaic 225-mm high speed CCD detector and processed with MOSFLM (38) and SCALA (39). The crystal belongs to space group P212121, with one complex per asymmetric unit. 5% of the reflections were used to calculate R_{free}. The structure was solved by molecular replacement, and AZD3839 was well defined in the difference electron density. REFMAC (40) and AUTOBUSTER (41) were used for crystallographic refinement, and Coot (42) was used for model building. X-ray data collection and refinement statistics are listed in Table 1.

hBACE1 and hBACE2 Time-resolved-FRET Assay—The procedure used has been described elsewhere (37). In short, the soluble part of the human β-secretase (recombinant hBACE1 enzyme, amino acids 1–460, or hBACE2 enzyme, amino acids 1–473) was mixed with compound in reaction buffer (sodium acetate, CHAPS, Triton X-100, EDTA, pH 4.5) and preincubated for 10 min. Substrate (Europium)CEVNLDAEFK(Qsy7) was added, and the reaction was allowed to proceed for 6.5 h in darkness under the lid at 22 °C until stopped with the addition of sodium acetate, pH 9. The fluorescence of the product was measured on a Victor II 1420 Multilabel Counter plate reader (Wallac) with an excitation wavelength of 340 nm and an emission wavelength of 615 nm.

Human Cathepsin D FRET Assay—Cathepsin D enzyme (Calbiochem) and substrate (Ac-Glu-Asp(EDANS)-Lys-Pro-Ile-Leu-Phe-Phe-Arg-Leu-Gly-Lys(DABCYL)-Glu-NH_2, where EDANS is 5-((2-aminoethyl)amino)naphthalene-1-sulfonic acid, and DABCYL is 4-([4-(dimethylamino)phenyl]azo)benzoic acid succinimidyl ester) (Bachem) were separately diluted in glycine-HCl buffer. Cathepsin D was mixed with compound dissolved in DMSO and preincubated for 10 min. Substrate was added, and the reaction mixture was incubated for 15 min in darkness at 22 °C. The fluorescent signal was measured on a Victor II 1420 Multilabel Counter plate reader (Wallac) with an excitation wavelength of 355 nm and an emission wavelength of 460 nm.

SH-SY5Y sAPPβ Release Assay—SH-SY5Y cells were cultured in DMEM/F-12 with Glutamax, 10% FCS, and 1% nonessential amino acids (Invitrogen). Compound was incubated with cells for 16 h at 37 °C, 5% CO_2. MSD plates (Meso Scale Discovery, Gaithersburg, MD) were used for the detection of sAPPβ release according to the manufacturer's instructions, and the plates were read in a SECTOR Imager. In addition, the cell plates were used to analyze cytotoxicity using the ViaLight™ Plus cell proliferation/cytotoxicity kit (Cambrex BioScience) according to the manufacturer's instructions.

SH-SY5Y Aβ40 Release Assay—The procedure used has been described elsewhere (37). In short, SH-SY5Y cells overexpressing APP695wt were cultured in DMEM/F-12 with Glutamax, 10% FCS, and 1% nonessential amino acids (Invitrogen). Compound was incubated with cells for 16 h at 37 °C, 5% CO_2 in cell culture medium. Invitrogen ELISA strips KHB3482 were used for the detection of human Aβ40 secreted into medium according to the manufacturer's instructions. The strips were read using a Spektramax microplate reader (Molecular Devices).

N2A Aβ40 Release Assay—N2A cells were cultured in minimum Eagle's medium with 10% FCS, 10 mM HEPES, Nonessential amino acids (Invitrogen), and Penicillin-Streptomycin (Invitrogen). The compound was incubated with cells for 16 h at 37 °C, 5% CO_2 in cell culture medium. Invitrogen ELISA strips KMB3481 were used for the detection of mouse Aβ40 secreted into medium according to the manufacturer's instructions. The strips were read using a Spektramax microplate reader (Molecular Devices).

Mouse Primary Neuron Aβ40 Release Assay—Primary cortical cells were isolated from fetal C57BL/6 mice (E16). The cortices were kept in calcium and magnesium free Earle's Balanced Salt Solution (CMF-EBSS) (Invitrogen) solution containing 0.25% trypsin and 2 units/ml DNase for 1 h at 37 °C and 5% CO_2. The cortices were washed in warm CMF-EBSS and gently triturated with flame-polished pipettes to separate the cells. The cell solution was transferred to a 50-ml Falcon tube containing medium (10% Ham's F-12, 10% fetal bovine serum, 1% 10 mM Hepes, 1% 2 mM L-glutamine, 0.5% 50 units/0.5 mg of penicillin-streptomycin, and 77.5% DMEM with 4.5 g/liter glucose) and filtered through a Cell Strainer 100 μm (BD Falcon). The cells were counted and plated onto 96-well poly-D-lysine-coated plates at a density of 200,000 cells/200 μl/well. After 5 days at 37 °C and 5% CO_2, the medium was changed to medium containing AZD3839 and a final concentration of 1% DMSO. After incubation overnight, the amount of released Aβ40 in the extracellular medium was measured using Invitrogen ELISA

strips KMB3481 according to the manufacturer's instructions. The strips were read using a Spektramax microplate reader (Molecular Devices). The cytotoxic effect of compounds was directly evaluated on the cell plates utilizing the ViaLight™ Plus cell proliferation/cytotoxicity kit (Cambrex BioScience) according to the manufacturer's instructions.

Guinea Pig Primary Neuron Aβ40 Release Assay—Primary cortical cells were prepared as described above. In brief, primary cortical cells were isolated from fetal Dunkin-Hartley guinea pigs (E25–27), and the amount of released Aβ40 in the extracellular medium was measured using Invitrogen ELISA strips KHB3482 according to the manufacturer's instructions.

Animals and Animal Handling, Rodents—Rodent experimentations were performed in accordance with relevant guidelines and regulations provided by the Swedish Board of Agriculture. The ethical permissions were provided by an ethical board specialized in animal experimentations (Stockholm North Animal Research Ethical Board). Female 11–14-week-old C57BL/6 mice (Harlan Laboratories, The Netherlands) were used. The mice ($n = 5–6$) received vehicle or AZD3839 at 80 and 160 μmol/kg (35 and 69 mg/kg, respectively) as a single dose or 100 μmol/kg (43 mg/kg) as repeated doses twice daily for 7 days via oral gavage. As vehicle, 5% dimethylacetamide and 20% hydroxypropyl-β-cyclodextrin in 0.3 M gluconic acid, pH 3, or 0.3 M gluconic acid, pH 3, alone were used. Male 4–9-week-old Dunkin-Hartley guinea pigs were purchased from HB Lidköping Kaninfarm (Sweden). The guinea pigs ($n = 6–8$) received vehicle or AZD3839 at 100 and 200 μmol/kg (43 and 86 mg/kg, respectively) as a single dose via oral gavage. As vehicle, 20% hydroxypropyl-β-cyclodextrin in 0.3 M gluconic acid, pH 3, was used. Animals were anesthetized 0.5, 1.5, 3, 4.5, 8, or 16 h after first or final administration of vehicle or drug and were then kept under isoflurane anesthesia. CSF was aspirated from the cisterna magna, and plasma was isolated from blood collected by cardiac puncture into EDTA tubes. Animals were then sacrificed by decapitation, and brains were dissected into hemispheres.

Animals and Animal Handling, Primates—The primate study was performed at Maccine Pte Ltd (Singapore), accredited by the Association for Assessment and Accreditation of Laboratory Animal Care International (AAALAC). An explorative study with few animals was performed in female 3–5-year-old cynomolgus (*Macaca fascicularis*) monkeys originally obtained from Indonesia. Animals were anesthetized and surgically prepared with indwelling cannulae inserted into the cisterna magna and connected to a subcutaneous access port to permit CSF sampling. The primates ($n = 3–4$) were restrained in primate chairs before dosing and were fully conscious during the dosing procedure. The dose was administered intravenously via an implanted cannula in the vena cava at a constant infusion rate of 10 ml/kg/h using a syringe pump over a 15-min period at a target dose volume of 2.5 ml/kg to achieve dose levels of 5.5 and 20 μmol/kg (2.4 and 8.6 mg/kg, respectively). As vehicle, 0.3 M gluconic acid, pH 3.89, was used. Blood and CSF samples were collected at −2 h pre-dose, −1 h pre-dose, and 0.25, 0.5, 1.5, 3, 4.5, 6, 8, 12, 16, and 24 h post-AZD3839 dose initiation. CSF was obtained using a Huber needle inserted into the subcutaneous port, and blood was collected from the femoral vein into EDTA tubes.

Extraction and Analysis of Aβ and sAPPβ in Animal Samples—The left brain hemispheres were homogenized in 0.2% diethylamine with 50 mM NaCl followed by ultracentrifugation. Recovered supernatants were neutralized to pH 8.0 with 2 M Tris-HCl. For mouse samples, Aβ40, Aβ42, and sAPPβ levels in brain extracts and Aβ40 levels in plasma were analyzed using commercial Aβ1–40 and Aβ1–42 ELISA kits (#KMB3481 and #KMB3441, Invitrogen) and an MSD sAPPβ kit (K110BTE-2 Meso Scale Discovery). For guinea pig samples, Aβ40 and Aβ42 levels in brain extracts, CSF, and plasma were analyzed using commercial Aβ1–40 (#KMB3481, Invitrogen) and Aβ1–42 (#80177 RUO, Innogenetics, Gent, Belgium) ELISA kits. The primate CSF samples were analyzed for Aβ40 and Aβ42 using the same ELISA kits as for the guinea pig samples. The primate CSF sAPPβ were analyzed using MSD sAPPβ kit (K111BTE-2 Meso Scale Discovery). To compensate primate CSF efficacy data for circadian rhythm variation, the two dose groups were compared with vehicle for each time point during data analysis.

Analysis of mouse and guinea pig Aβ data were performed using Prism 4 (GraphPad) with one-way analysis of variance followed by Dunnett's or Bonferroni's Multiple Comparison Test. The level of significance was set at $p < 0.05$. Primate CSF data were analyzed using a linear mixed model with treatment group, time, interaction between treatment and time, and mean base line as fixed effects and subject as a random effect; to take account of the repeated measurements, structure was fitted to each outcome variable separately, using proc mixed in the SAS software. For each time point, the two dose groups were compared with vehicle within the model. Before analysis, a log transform was applied to the data. No correction for multiplicity was performed that increased the risk of finding false positives. The level of significance was set at $p < 0.05$.

Bioanalysis of in Vivo Samples—Bioanalysis was performed as previously described in Borgegard *et al.* (43). Briefly, right brain hemisphere was homogenized in 2 volumes (w/v) of Ringer solution. Aliquots of plasma (25 μl) and brain homogenate (50 μl) were precipitated with 150 μl of acetonitrile containing a generic internal standard (200 nmol/liter warfarin). Samples were mixed, centrifuged, appropriately diluted with mobile phase, and analyzed on a LC-MS/MS system. CSF aliquots (15 μl) were directly diluted and injected. Correction for blood content in brain was made by subtracting 1.3% of the plasma concentration from the total brain concentration.

Binding to Plasma Proteins and Brain Tissue—Plasma protein and brain tissue binding was determined as described in Borgegard *et al.* (43). In short, AZD3839 was added to mouse, guinea pig, and monkey plasma to a final concentration of 10 μM. An aliquot was transferred to a dialysis plate with phosphate buffer on the other site and incubated for 18 h at 37 °C. Proteins were removed from aliquots (50 μl) of plasma and buffer samples, internal standard was added, and proteins were analyzed with LC-MS/MS. The unbound fraction in plasma was calculated from the ratio of the MS-area of AZD3839 in buffer divided by sum of the areas of AZD3839 in buffer and plasma. Recovery and stability in plasma was controlled for.

To determine brain tissue binding, 300-μm-thick coronal rat brain slices were incubated for 5 h in 10 ml of an artificial interstitial fluid buffer containing 1 μM of AZD3839. After the incu-

bation, slices were weighted and homogenized, proteins were removed, and LC-MS/MS analysis was performed. The unbound fraction in brain was calculated as described in Fridén *et al.* (44). Mouse and guinea pig total brain concentrations were converted to free concentrations by multiplying with the unbound fraction. It has been shown that this unbound fraction in brain is inter-exchangeable between different species (45).

PKPD Analysis—Inspection of the time course of the concentration of AZD3839 and time course of the changes in Aβ40 concentration in CSF and brain revealed hysteresis, *i.e.* the drug-mediated response was delayed compared with drug concentrations. Therefore, a turnover model (46) was selected to analyze the observed exposure and Aβ40 time response data. The indirect response model assumes that the base-line Aβ40 level under physiological conditions is governed by a zero-order generation process and a first order clearance process according to the equation.

$$\frac{d[A\beta40]}{dt} = K_{in} \times \text{Effect} - k_{out} \times [A\beta40] \qquad \text{(Eq. 1)}$$

The Effect parameter in Equation 1 represents the inhibitory activity of AZD3839 on the production rate (K_{in}) that was described with an inhibitory sigmoidal concentration-effect relationship as expressed in Equation 2. The K_{in} was assumed to be equal to product of the Aβ40 concentration at base-line $[A\beta40]_0$ and the first order turnover rate constant k_{out}.

$$\text{Effect} = 1 - \frac{E_{max} \times C}{IC_{50} + C} \qquad \text{(Eq. 2)}$$

in which E_{max} is the maximum effect, IC_{50} is the concentration at 50% of maximal effect, and C is the observed plasma concentrations. Because a constant ratio existed between brain or CSF and plasma levels in mouse and guinea pig, all effects were related to plasma concentrations.

As the Aβ40 concentration could only be measured once in each animal, no information on the individual Aβ40 base-line value could be obtained. It was assumed that all animals that were sacrificed at the same time point had a base-line value equal to the median Aβ40 concentration in the vehicle group for that time point. Hence, for each time point different Aβ40 base-line values were estimated from the data.

Time response data were analyzed by means of a population or mixed-effects modeling approach using NONMEM Version 7.2.0 (ICON development services, Hanover, MD). The first-order conditional estimation method with interaction was used for estimation. The modeling process was guided by statistical and visual checks, such as the visual predictive check (47), which was used to evaluate if the identified model is able to predict the observed variability for 80% of the population in the data that were used for model identification. By means of a Monte Carlo simulation, 1000 hypothetical datasets are simulated using the estimated model parameters and variability and uncertainty distributions and experimental conditions (*i.e.* dosing, duration). The distribution (median and 10th and 90th percentiles) of the simulated data were compared with the distribution of the observed values in the original dataset. Differences and overlap of the simulated and original distributions indicated the accuracy of the identified model.

RESULTS

Discovery and Optimization of Amidine-containing BACE1 Inhibitors Leading to AZD3839—A fragment-based lead generation approach was undertaken with the aim to find small molecule BACE1 inhibitors. Compound **1** (48), containing the amidine binding motif, was a hit in a one-dimensional NMR screen and was chosen for further development into lead compounds as shown in Fig. 1. Compound **1** was developed into a series of dihydroisocytosine compounds with sub-micromolar potency as exemplified by compound **2** (49). Simultaneously, our efforts were directed toward development of the aminohydantoin series (Compound **3**) (50–51) containing the same amidine binding motif. Further scaffold hopping via the bicyclic aminoimidazole **4** (37) led us to the isoindole series, from which compound **5** (52) represents an early compound. With focus on improving the low permeability and lack of brain exposure that were major drawbacks with compounds **4** and **5**, we found the fluoro-isoindoles, in which the amidine is "shielded" from the environment by a combination of electronic and steric effects. In addition to a reduced pK_a, we reasoned that a weak internal hydrogen bond could be formed between the fluoro atom and the exocyclic amine. In this way, the effective number of displayed hydrogen bond donors in the molecule was reduced. This shielding resulted in a significant increase in permeability (Fig. 1) and a reduction of the P-glycoprotein multidrug transporter-related efflux ratio to 10 for compound **6** (52) compared with >35 for compound **5** (52) as determined with MDR1-overexpressed cells. During lead optimization, the inherently high pK_a of the amidine in the isoindoles **5** and **6** was further reduced by incorporation of electron withdrawing substituents as in compound **7** (53). CNS exposure of compound **7** was high, the *in vitro* efflux ratio was 3.5, but the potency for inhibition of BACE1 declined compared with compound **5**. Reducing the molecular weight and lipophilicity of the substituent by replacement of CF_3 with CHF_2 gave AZD3839 with restored potency and also a high ligand-lipophilicity efficiency ($pIC_{50} - \log P = 5.60$) and an efflux ratio of 3.5.

Crystal Structure of AZD3839 in BACE1 Active Site—AZD3839 was soaked into crystals of BACE1, and the resulting crystal structure was refined to 1.8 Å resolution (Fig. 2, Table 1). AZD3839 binds to BACE1 in a flap-open conformation with the pyridine nitrogen located close to the S2 pocket, interacting with Trp-76 via an important hydrogen bond. The difluoromethyl substituent *ortho* to the pyridine nitrogen is in a subpocket of the active site and displaces a conserved water molecule normally coordinated by Ser-35 and Asn-37. As expected, the amidine group of the ligand interacts with the catalytic aspartates, Asp-32 and Asp-228. The S1 pocket is occupied by the hydrophobic phenyl ring, and the pyrimidine ring is placed in the S3 pocket. One of the water molecules coordinating the pyrimidine nitrogens is buried in the S3 subpocket. It acts as a water bridge between ligand and protein by donating a hydrogen bond to the carbonyl of Ser-229. The structure activity relationship of AZD3839 and related analogues (54) as well as the development of the synthesis of the compound into a scalable route[3] will be discussed elsewhere.

In Vitro Pharmacology of AZD3839—The potency of AZD3839 to inhibit BACE1 and its closely related enzymes was

[3] A. Minidis, unpublished data.

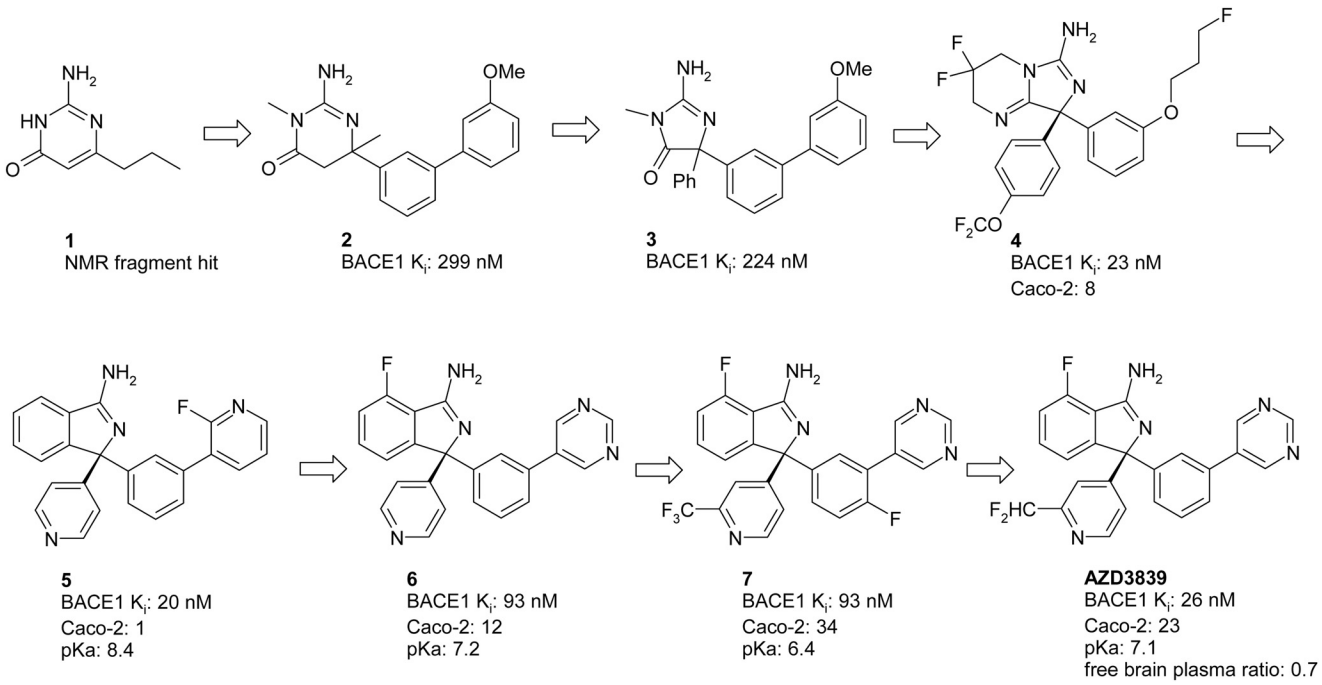

FIGURE 1. **Discovery and optimization of amidine-containing BACE1 inhibitors leading to the *in vivo* compound AZD3839.** BACE1 K_i values were determined *in vitro* using a FRET protocol. Caco-2 permeability from A-B was determined as Apparent permeability (P_{app}) values (10^{-6} cm/s) at pH 6.5. Free brain plasma ratio was calculated from brain and plasma exposures from *in vivo* experiments in C57BL/6 mice. The fraction unbound in brain and in plasma was determined in separate experiments.

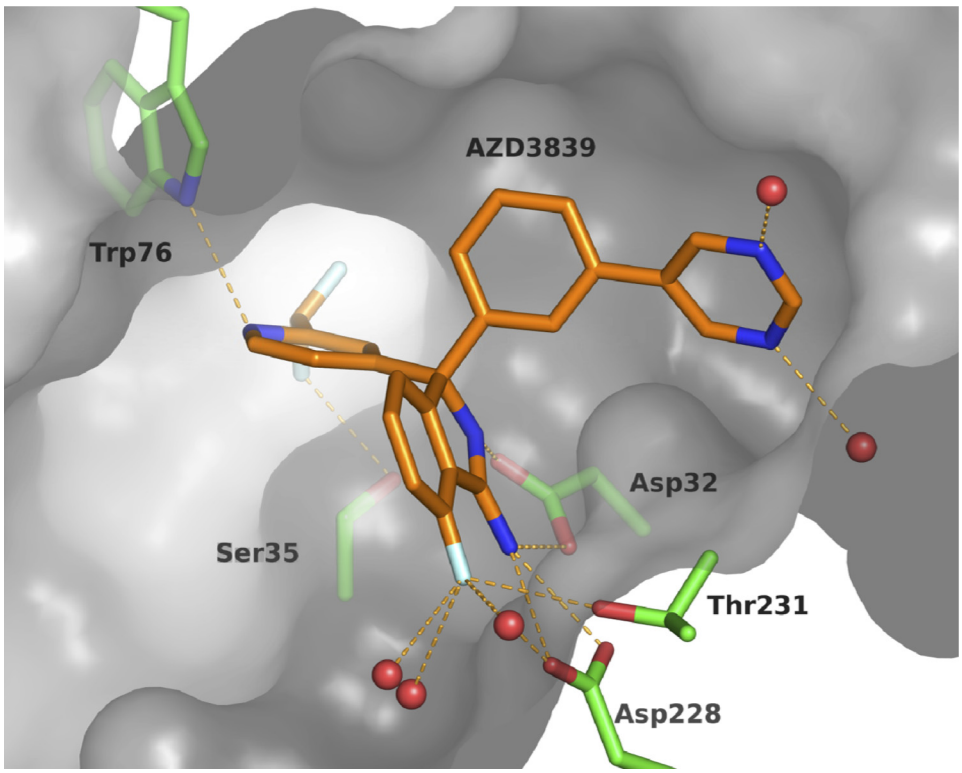

FIGURE 2. **AZD3839 binding in the active site of BACE1, PDB ID code 4b05.** Key interactions between AZD3839 (*orange*) and BACE1 (*green*) are highlighted. Water molecules depicted as *red spheres*. The protein surface is shown in *grey* (flap partly removed for clarity). The figure prepared using PyMOL (68).

evaluated *in vitro* (Table 2). In a concentration-dependent manner, AZD3839 reached 100% inhibition of recombinant human BACE1 cleavage of a 10-amino acid-long swe-mutation APP sequence, with a resulting K_i of 26.1 nmol/liter. The potency to inhibit BACE2 was 14-fold higher (K_i = 372 nmol/liter). AZD3839 showed more than a 1000-fold selectivity against the aspartic protease cathepsin D (K_i>25 μmol/liter). In SH-SY5Y cells overexpressing APP695wt, AZD3839 effi-

ciently decreased the Aβ40 levels in a concentration-dependent manner with a resulting IC_{50} of 4.8 nmol/liter. AZD3839 also efficiently decreased the formation of sAPPβ in SH-SY5Y cells with an IC_{50} of 16.7 nmol/liter. In a similar fashion AZD3839 decreased the Aβ40 levels secreted from C57BL/6 mouse primary cortical neurons, N2A cells (mouse neuroblastoma), and Dunkin-Hartley guinea pig primary cortical neurons, resulting in IC_{50} values of 50.9, 32.2, and 24.8 nmol/liter, respectively. Hence, based on Aβ40 readout, AZD3839 was nine times more potent in the human cell assay compared with the average of the two mouse cellular assays.

Plasma Protein and Brain Tissue Binding—The *in vitro* plasma protein binding of AZD3839 was determined by equilibrium dialysis in mouse, guinea pig, and monkey. The *in vitro* unbound fractions were 3.2 ± 0.2, 20 ± 1.1, and 6.9 ± 0.8% for mouse, guinea pig, and monkey, respectively. AZD3839 was found to be stable in plasma for at least 24 h. The free fraction in brain tissue was 7.9%.

Inhibition of Aβ Generation in Mouse—In C57BL/6 mice, orally administrated AZD3839 gave a dose- and time-dependent reduction of plasma and brain Aβ (Fig. 3). Brain concentrations of AZD3839 increased rapidly and peaked at 0.5 h after dosing 80 μmol/kg AZD3839, the earliest observation time point. Brain Aβ40 levels decreased ~30% *versus* vehicle at 1.5 h after dose and returned to base line after 4.5 h. A higher dose of AZD3839 (160 μmol/kg) led to increased brain concentrations and consequently a more pronounced and long-lasting reduction (~50% *versus* vehicle) that returned to base line after 8 h (Fig. 3*A*). The levels of brain Aβ42 (Fig. 3*B*) and sAPPβ (not shown) followed the same pattern as Aβ40. In addition, both doses of AZD3839 reduced plasma levels of Aβ40 by ~60% *versus* vehicle over a prolonged period (Fig. 3*C*). At 8 h after administration, the inhibitory effect started to decline within the low dose group, whereas maximal efficacy was maintained within the high dose group. Sub-chronic administration of 100 μmol/kg AZD3839 twice daily to C57BL/6 mice for 7 days demonstrated comparable efficacy on brain and plasma Aβ40 to a single administration (not shown).

Inhibition of Aβ Generation in Guinea Pig—The concentration- and time-dependent reduction of plasma, brain, and CSF Aβ in guinea pigs was investigated between 0.5 and 16 h after an oral dose of 100 or 200 μmol/kg AZD3839. Brain Aβ40 was reduced up to 8 h after the dose in animals receiving the higher dose (~20–60% *versus* vehicle), whereas guinea pigs receiving the lower dose demonstrated a reduction at 1.5–4.5 h after dose (~20–30% *versus* vehicle) (Fig. 4*A*). AZD3839 at 200 μmol/kg reduced CSF Aβ40 levels by 50% at 3 h after dose (Fig. 4*C*). The CSF Aβ40 levels were still reduced by 40% at 8 h after dose, although the reduction failed to reach statistical significance at this later time point. In addition, the doses tested reduced the plasma levels of Aβ40 by ~30–80% *versus* vehicle over the entire period (Fig. 4*E*). The levels of Aβ42 in brain, CSF, and plasma followed the same pattern as Aβ40, with a statistically significant concentration- and time-dependent decrease after treatment with AZD3839 (Fig. 4, *B*, *D*, and *F*). The reduction of both Aβ species was similar in brain and CSF. The decrease of Aβ in plasma preceded the central effect and was sustained for a longer time (Fig. 4, *G* and *H*).

Inhibition of Aβ Generation in Non-human Primates—Despite a large variation in the basal (pre-dose) CSF levels of Aβ40, Aβ42, and sAPPβ in the cynomolgus monkeys in an explorative study, an intravenous infusion of 20 μmol/kg AZD3839 significantly reduced the levels of Aβ40, Aβ42, and sAPPβ in CSF between 3 and 12 h after dose (Fig. 5, *A*–*C*). The inhibitory effect on sAPPβ was more pronounced than the effect on Aβ40 and Aβ42, and AZD3839 demonstrated an unexpected long

TABLE 1
X-ray data collection and refinement statistics

	BACE1 complex with AZD3839
Data collection	
Space group	$P2_12_12_1$
Unit cell dimensions	
Å	$a = 47.53$, $b = 76.53$, $c = 104.16$
Degree	$\alpha = 90.0$, $\beta = 90.0$, $\gamma = 90.0$
Resolution range (Å)[a]	26.3-1.8 (1.85-1.80)
No. of observations	120,237
No. of unique reflections	35,173
Data redundancy[a]	3.4 (3.3)
Data completeness (%)[a]	97.9 (94.1)
$\langle I/\sigma(I)\rangle$[a]	20.8 (2.3)
R_{merge} (%)[a,b]	4.7 (49.1)
Refinement	
Resolution range (Å)[a]	26.3–1.8 (1.85–1.80)
R_{work} (%)[a]	17.8 (34.0)
R_{free} (%)[a]	21.5 (35.4)
Wilson *B*-factor (Å^2)	24.0
Overall mean *B*-factor (Å^2)	26.9
No. of atoms	
Protein atoms	2921
Heterogen atoms	409
Solvent atoms	356
Root mean square deviation values	
Bond lengths (Å)	0.010
Bond angles (°)	1.13
Ramachandran statistics[b] (%)	
Most favored + additional allowed	99.7
Generously allowed	0.3

[a] Numbers in parentheses refer to the highest resolution shell.
[b] Ramachandran statistics are from PROCHECK (69).

TABLE 2
AZD3839 potency against BACE1, related aspartic proteases, and cellular APP processing assays
Data are reported as the mean ± S.E. of 4–11 independent experiments.

Study	Results (pK_i or pIC_{50} ± S.E.)
	nmol/liter
hBACE1 affinity, TR-FRET (K_i, nmol/liter)	26.1 ($pK_i = 7.58 \pm 0.02$), $n = 6$
SH-SY5Y/APP, Aβ40 readout (IC_{50}, nmol/liter)	4.8 ($pIC_{50} = 8.32 \pm 0.03$), $n = 11$
N2A, Aβ40 readout (IC_{50}, nmol/liter)	32.2 ($pIC_{50} = 7.49 \pm 0.11$), $n = 5$
SH-SY5Y, sAPPβ readout (IC_{50}, nmol/liter)	16.7 ($pIC_{50} = 7.78 \pm 0.04$), $n = 9$
Mouse primary neurons, Aβ40 readout (IC_{50}, nmol/liter)	50.9 ($pIC_{50} = 7.29 \pm 0.05$), $n = 7$
Guinea pig primary neurons, Aβ40 readout (IC_{50}, nmol/liter)	24.8 ($pIC_{50} = 7.67 \pm 0.09$), $n = 9$
Selectivity targets	
hBACE2 affinity, TR-FRET (K_i, nmol/liter)	372.4 ($pK_i = 6.43 \pm 0.07$), $n = 4$
hCathepsin D affinity, TR-FRET (K_i, nmol/liter)	>25,000 ($pK_i < 4.6$), $n = 4$

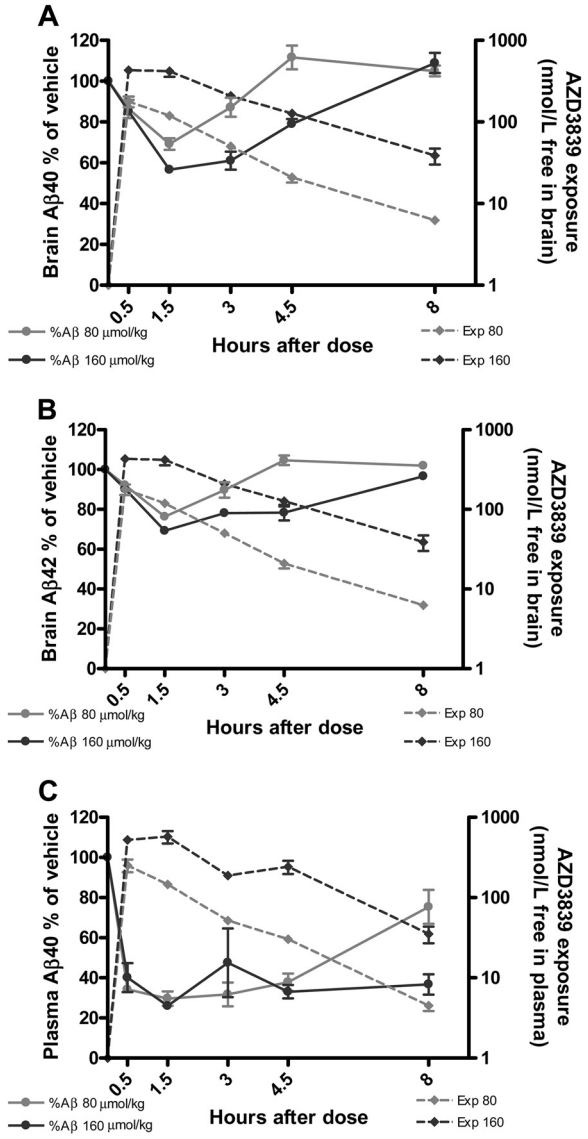

FIGURE 3. **Time- and dose-dependent inhibition of Aβ in C57BL/6 mice.** Pharmacologic effects *in vivo* of oral administration of AZD3839 to C57BL/6 mice AZD3839 demonstrated a time- and concentration-dependent reduction of Aβ40 (*A*) and Aβ42 (*B*) in brain and Aβ40 in plasma (*C*). Data are expressed as % of vehicle Aβ levels (mean ± S.E.; $n = 5–6$ per group).

delay in the onset of effect. A lower dose of AZD3839 (5.5 μmol/kg) demonstrated statistically significant effects on the levels of Aβ40 and Aβ42 at 4.5 h after dose only. However, at the lower dose of AZD3839 there was no effect on sAPPβ levels in CSF, possibly due to the low exposure of AZD3839 and the half-life of the sAPPβ peptide in CSF. Drug concentration in CSF peaked at the end of the infusion (15 min) and had already decreased 10-fold after 3 h (Fig. 5*D*). In CSF samples from animals receiving the lower dose, the concentration levels were below the limit of quantification of the assay (3 nmol/liter), from 4.5 h after dose onwards. A simultaneous fit of the plasma AZD3839 concentrations observed after the 5.5 and 20 μmol/kg intravenous infusions using a 2-compartment model yielded a compound half-life estimate in plasma of 18 min. In addition, the effect with the higher dose did not seem to return back to base line during the time period tested.

Exposure Correlations—Fig. 6 shows the correlation between free concentrations of AZD3839 measured in plasma, CSF, and brain of the various studied preclinical species. All measured exposure samples from all dose groups have been included as long as concentrations were above the limit of quantification. Equilibrium between the different compartments in mouse and guinea pig was rapidly achieved and maintained, as judged by their linear relationship and steepness approaching 1. The ratio between free concentrations in plasma and brain in mouse was 0.7, the average of the observed individual free brain plasma ratios, which indicated unrestricted access into the CNS of AZD3839. A right-shift of the plasma-brain correlation in guinea pig was seen compared with mouse (Fig. 6*A*), which pointed to more restricted access to the brain. Also, in the CSF of guinea pig, AZD3839 levels were lower compared with plasma (Fig. 6*B*). However, the concentration in CSF appeared higher than free levels in brain (Fig. 6*C*). CSF values were not corrected for binding. In primate the correlation between free plasma and CSF concentrations was more shallow (slope = 0.59), indicating that clearance in the CSF compartment was slower than in plasma (see also Fig. 5*D*). At early time points a large difference was observed between the plasma and CSF concentrations, whereas at later times levels in the two compartments were similar.

PKPD Modeling of the Inhibition of Aβ Generation in Mouse and Guinea Pig—A PKPD analysis was performed to quantify the *in vivo* potency of the reduction of Aβ40 in plasma, CSF, and brain in mouse and guinea pig. All effects were related to plasma concentrations of AZD3839. The change in the Aβ40 levels in plasma, CSF, and brain was best described with a turnover model, in which AZD3839 inhibits the zero-order production rate with a sigmoidal E_{max} relationship. The parameter estimates are summarized in Table 3, and the simulated concentration-effect relationships under steady state conditions are shown in Fig. 7. The IC_{50} values to reduce Aβ40 in plasma were 64- and 48-fold lower than for the brain for mouse and guinea pig, respectively. Also, the turnover half-life of the peripheral effect was lower in both species compared with the half-life of the central effects. As the equilibrium between plasma and brain concentrations are rapidly achieved, this shows that the effects in the brain occur at a slower pace.

DISCUSSION

In this report we describe the discovery of AZD3839, a potent and selective orally bioavailable small molecule BACE1 inhibitor. Based on the preclinical profile, AZD3839 may have therapeutic potential in the treatment of AD. AZD3839 was developed with a fragment-based lead generation and structure-based design approach. The use of PKPD modeling has increased our understanding of the quantitative relationship between concentrations of AZD3839 and its efficacy on Aβ reduction. Moreover, it was used for clinical dosing regimens targeting anticipated clinically relevant reductions of brain Aβ. Based on the overall pharmacological profile reported in this manuscript and its drug like properties, AZD3839 was progressed into Phase 1 clinical trials in man.

A major struggle with the development of BACE1 inhibitors has been the demonstration of robust *in vivo* pharmacological effect. Loss of potency in cellular systems, low bioavailability,

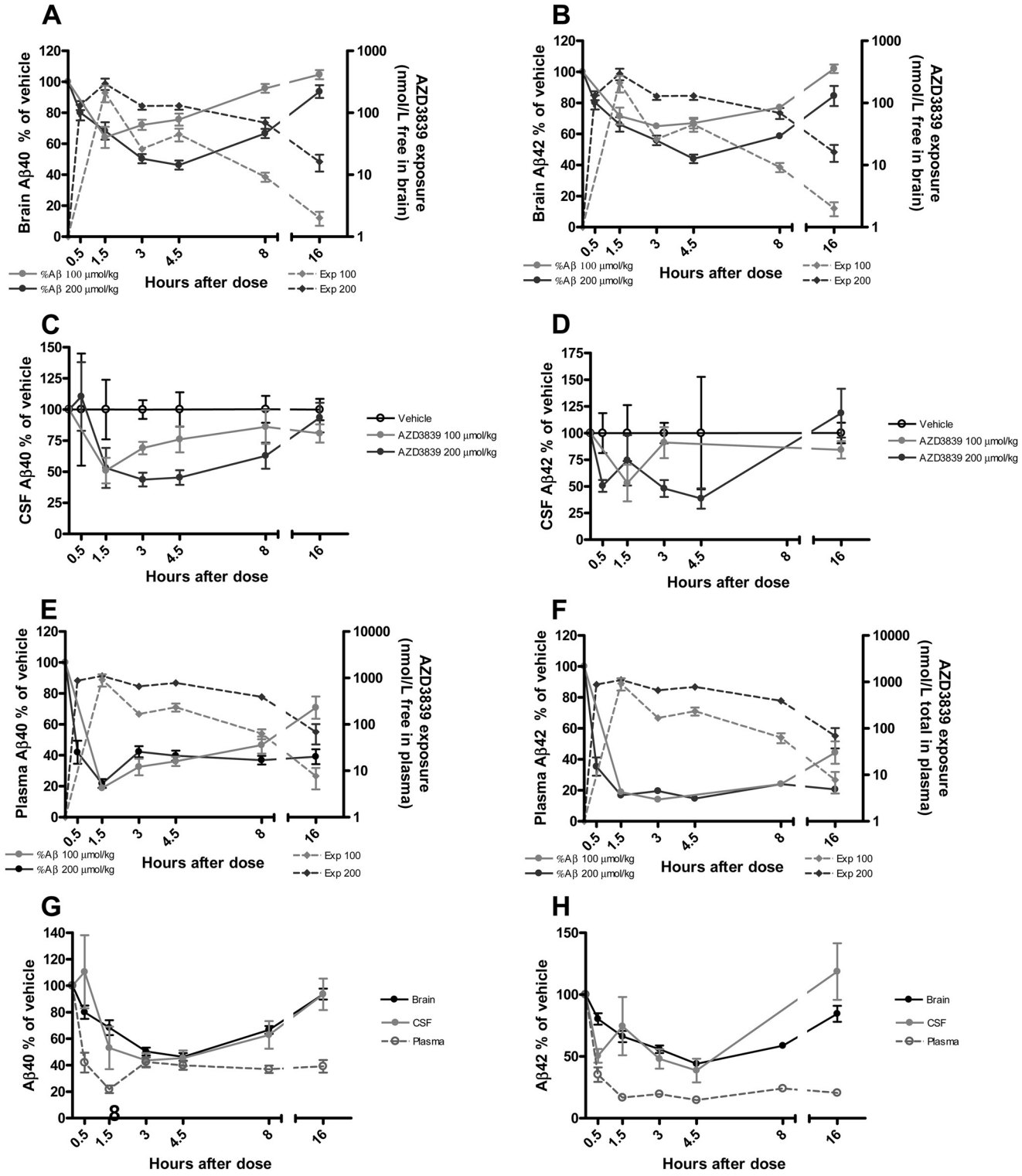

FIGURE 4. **Time- and dose-dependent inhibition of Aβ generation in guinea pig.** In guinea pig, orally administrated AZD3839 reduced Aβ40 (*left panels*) and Aβ42 (*right panels*) in a time- and dose-dependent manner in brain (*A* and *B*), CSF (*C* and *D*), and plasma (*E* and *F*). The effect in plasma was more pronounced than the effect in brain and CSF. Effects in brain and CSF had similar time-response and extent at the measured time points (*G* and *H*). Data are expressed as % of vehicle Aβ levels (mean ± S.E.; $n = 6–8$ per group).

and particularly affinity for efflux transporter systems at the blood-brain barrier level has been offered as explanations (33–35). Because potency on BACE1 and free concentration at the target site are the single determinants to provide *in vivo* pharmacological efficacy, the strategy has been to maximize permeability and control active transport out of the CNS. With AZD3839 we were able to combine these properties with a high cellular potency, good brain-to-plasma ratios, and robust pharmacological effect in three preclinical species including non-human primates.

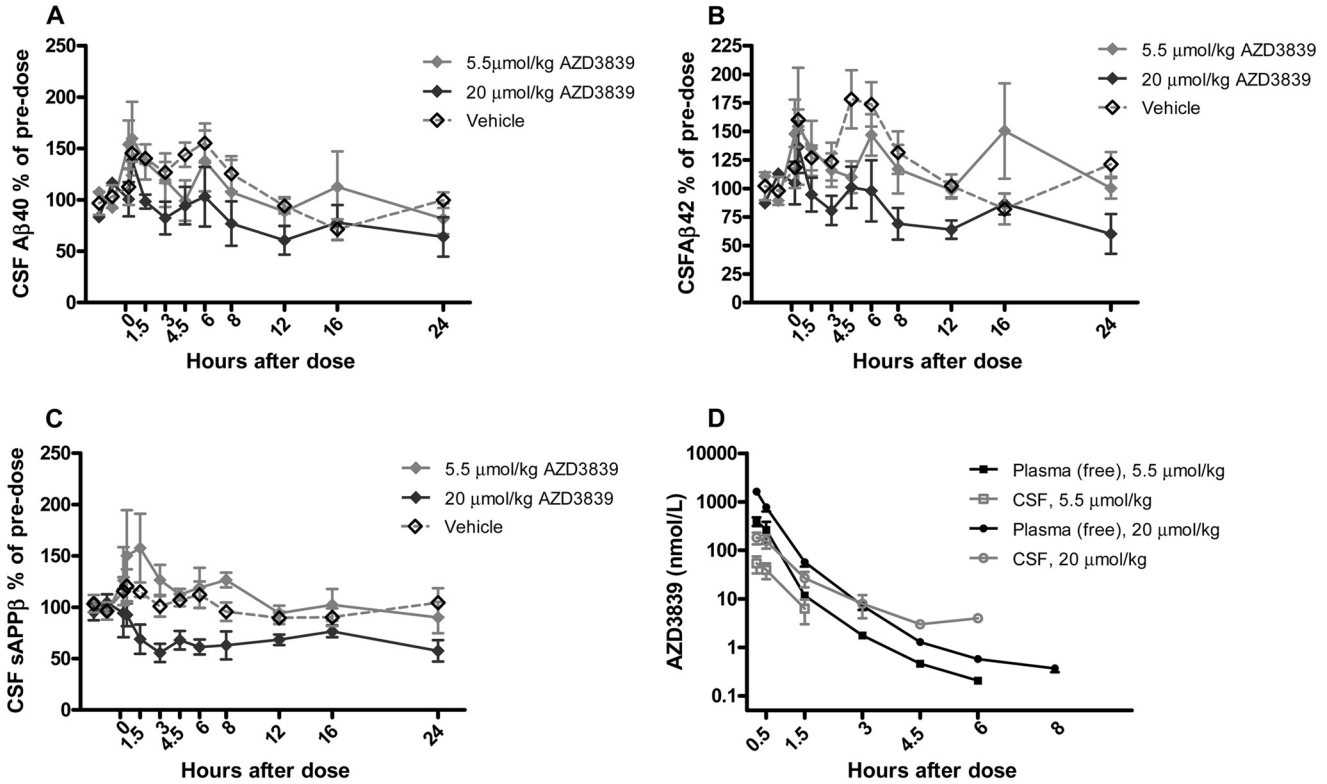

FIGURE 5. **Time- and dose-dependent inhibition of Aβ generation in non-human primates.** In cynomolgus monkeys, AZD3839 reduced CSF Aβ40 (*A*), Aβ42 (*B*), and sAPPβ (*C*) time- and dose-dependently after a single 15-min intravenous infusion. *D*, the pharmacokinetic profile of AZD3839 showed that concentrations of AZD3839 in plasma and CSF peaked upon cessation of the infusion. Data are expressed as % of pre-dose Aβ levels or AZD3839 concentration (mean ± S.E.; vehicle $n = 4$, and AZD3839-treated $n = 3$ per dose).

For many analogues from the same chemical series as AZD3839, an excellent correlation between primary neurons and human SH-SY5Y cells has been established (55). Also, a correlation has been found between mouse and guinea pig *in vitro* primary neuron potency and *in vivo* potency on central Aβ40 reduction (55). Although the cellular potency is lower than the *in vivo* potency, the ratio between the values is approximately similar between compounds and species (see also Ref. 56). For AZD3839, the ratio between potency measured in primary neurons and *in vivo* efficacy is 5- and 7-fold for mouse and guinea pig, respectively, after correction for the concentration difference between plasma and brain. This increased the confidence that BACE1 inhibition in this human, neuronal-derived, cell line produced meaningful data for screening and optimization of novel BACE1 inhibitors. The ability to predict *in vivo* pharmacological outcome based on *in vitro* data possibly combined with early pharmacokinetic studies strongly reduced the number of preclinical *in vivo* effect studies.

Aβ and sAPPβ have been established as relevant biomarkers that reflect BACE1 activity and have been exploited to establish translational relationships between the different cellular assays and animal models. In this work, mice, guinea pigs and non-human primates were used to assess Aβ reduction with BACE1 inhibitors. We made use of wild-type animals, which express wild-type APP and BACE1, and the non-mutated variants of the γ -secretase complex. This allows for interfering with components of the amyloid pathway in their native forms and natural setting and reflects the endogenous situation. Results from this model could, therefore, be generalized to the wider population of cases of sporadic AD. In addressing BACE1 inhibition, this is of particular importance as many of the transgenic mouse models of cerebral amyloidosis overexpress APP carrying the Swedish mutation. The Swedish mutation increases BACE1 processing of APP, and this increased affinity for the substrate caused by the mutation results in BACE1 inhibitors reduced potency, a limitation of the models overexpressing APPswe (APP carrying the Swedish mutation) (11).

Guinea pigs, non-human primates, and humans have identical protein sequence homology for Aβ-peptides and are considered to be useful translational models (57, 58). In addition, studies have shown that drug transport into the CNS may be more similar between humans and primates (59, 60). Hence non-human primates will give an indication of the expected distribution to CSF of AZD3839 in humans.

Studies with γ-secretase and β-secretase inhibitors have demonstrated that the maximal drug concentration in brain and CSF often occurs later compared with the peak concentration in plasma (in-house observations). Moreover, Aβ reduction in brain and CSF is observed with even further delay (60). Therefore, it is important to perform time-response studies to understand the PKPD relationship and to obtain guidance on the optimal timing of single CSF sampling in studies in man. The observed delay in the Aβ lowering effect of AZD3839 is expected due to the time it takes for the compound to reach the target from the plasma compartment, Aβ not being the direct product of BACE1 inhibition and Aβ reduction being dependent on its clearance.

AZD3839 was able to completely abolish Aβ40 and sAPPβ production *in vitro*. In our preclinical animal models, however, the concentration-effect relationship of Aβ40 reduction revealed that AZD3839 achieved a maximal inhibition of ~60–70%, with the exception of the brain compartment in guinea pig (Fig. 7). Repeated dosing of AZD3839 in mouse did not alter this relationship; no tolerance or sensitization to the Aβ40 lowering in the brain was observed. Because the clearance of AZD3839 in mouse was relatively rapid, and the effect on Aβ40 reduction in brain had returned to base line after 6–8 h (Fig. 3), it was not surprising that no additional Aβ lowering was observed after sub-chronic dosing. Other groups have also reported that β- and γ-secretase inhibitors were not able to fully inhibit Aβ production in preclinical species in plasma and/or brain, although this might be compound-specific (56, 61, 62).

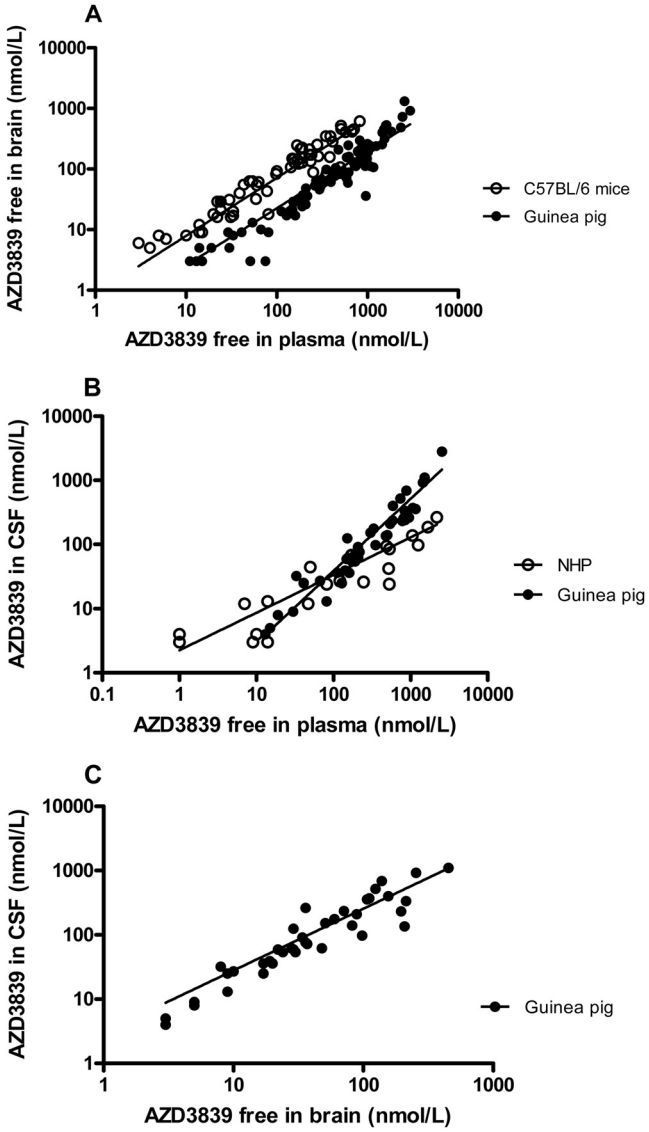

FIGURE 6. **Correlation between free plasma and free brain levels of AZD3839 in preclinical species.** All exposure data obtained collected at different times and treated with different doses of AZD3839 have been compiled. *A*, AZD3839 showed a constant free brain/plasma ratio over time and concentration range of 0.7 and 0.3 in C57BL/6 mice and guinea pig, respectively (mouse: $R^2 = 0.78$, slope = 0.96; guinea pig: $R^2 = 0.68$, slope = 0.94). *B*, AZD3839 showed a constant free CSF/plasma ratio over time and concentration range of 0.7 in guinea pig ($R^2 = 0.76$, slope = 1.1). AZD3839 showed time dependencies in the CSF exposure relative to plasma in non-human primates (*NHP*) ($R^2 = 0.75$, slope = 0.59). *C*, AZD3839 showed a constant free CSF/brain ratio over time and concentration range of 2.5 in guinea pig ($R^2 = 0.76$, slope = 0.96).

Aβ40 reduction in brain had returned to base line after 6–8 h (Fig. 3), it was not surprising that no additional Aβ lowering was observed after sub-chronic dosing. Other groups have also reported that β- and γ-secretase inhibitors were not able to fully inhibit Aβ production in preclinical species in plasma and/or brain, although this might be compound-specific (56, 61, 62).

The involvement of BACE1 in the processing of other substrates with biological significance could potentially cause adverse target-related effects with inhibition of BACE1. However, in 1-month rodent and dog toxicology studies, we have no indication this would be the case for AZD3839 (not shown).

In a clinical setting, plasma and CSF are the accessible compartments to measure soluble Aβ levels to determine target engagement. Therefore, it is important to establish if and how plasma or CSF levels relate to changes in brain Aβ levels. In mouse and guinea pig AZD3839 decreased Aβ levels in plasma at lower concentrations compared with the brain even after correction for differences in exposure. This may also have been observed for other β- and γ-secretase inhibitors in different preclinical species (30, 62, 63) but not all (56, 63). The reason for this is not entirely understood. AZD3839 might have difficulties to reach specific cellular compartments. The blood/plasma ratio was 0.8, which excluded that AZD3839 accumulated in blood cells. Based on these observations, a significant peripheral effect in human would be needed before central effects are expected. Importantly, in guinea pigs Aβ was similarly decreased by AZD3839 treatment in brain and CSF. This additionally strengthens the idea that CSF biomarkers are useful for the prediction of Aβ changes in the brain and that it is important to take CSF samples in early clinical testing to guide dosing and duration of human proof of mechanism (PoM) studies (64).

The potential of BACE1 inhibition as an AD-modifying drug target in humans is supported by BACE1 inhibitors that were reported to lower CSF Aβ40 and Aβ42 in healthy volunteers. Late in 2011, May *et al.* (30) showed in a single ascending dose study in healthy volunteers that the BACE1 inhibitor LY2811376 led to a maximum reduction of 80 and 60% in plasma and CSF Aβ40, respectively. At the American Academy of Neurology meeting in April 2012, Merck reported that the BACE1 inhibitor MK-8931 was able to lower CSF Aβ levels by

TABLE 3

AZD3839 PKPD parameter estimates

Summary of the parameter estimates (population mean (coefficient of variance %)) of the PKPD analysis of the AZD3839-mediated inhibition of Aβ40 in plasma, brain, and CSF in mouse and guinea pig. The potency values are expressed relative to the plasma concentration of AZD3839.

	Aβ40 reduction in mouse		Aβ40 reduction in guinea pig		
	Plasma	Brain	Plasma	Brain	CSF
	%		%		
E_{max} (%)	61 (44)	71 (72)	66 (27)	98 (123)	73 (64)
Unbound IC_{50} (nM)	5.9 (21)	380 (6)	12 (11)	578 (3)	260 (9)
Turnover half-life (h)	0.02 (4)	0.52 (19)	0.56 (99)	0.84 (12)	0.74 (48)

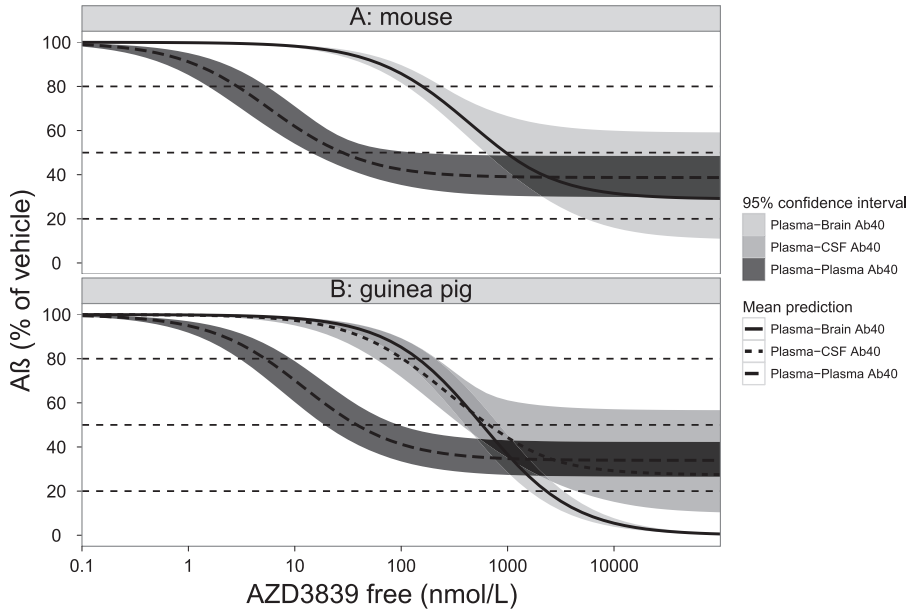

FIGURE 7. **PKPD analysis results of the reduction of Aβ40 after oral administration of AZD3839 to mouse and guinea pig.** The free plasma concentration-effect relationships of Aβ40 inhibition in mouse plasma and brain (*A*) and guinea pig plasma, CSF, and brain (*B*) using a population modeling approach are shown. The average parameter estimates are presented in Table 3. The *shaded areas* represent the prediction intervals for the different relationships on the basis of the estimated uncertainty in E_{max} and EC_{50} reported in Table 3.

more than 90% after 2 weeks of administration in healthy volunteers.

Biphasic concentration-effect relationships for Aβ reduction have been described for γ-secretase inhibitors Semagacestat, Avagacestat, Begacestat, and MK0752 in mice, rats, monkey, and human plasma (56, 65, 66). On CSF Aβ levels, less pronounced or no rise were observed for γ-secretase inhibitors in preclinical models, whereas the clinical data have been difficult to interpret due to limited data and drift in the base line. In contrast, AZD3839 did not show any sign of significant plasma or CSF Aβ rise above the concurrent vehicle control levels. Neither has this been reported for LY2811376 in preclinical species or human (30, 61).

Amyloid deposition occurs long before the patient begins to present symptoms (67). A key challenge in the field is that the optimal level of Aβ reduction has not yet been established for anti-amyloid therapy for AD. Also, amyloid deposition is believed to act as a trigger for the neurodegeneration in Alzheimer, but evidence suggests that this may not be directly linked to subsequent disease progression. Anti-amyloid therapies such as BACE1 inhibitors may, therefore, need to be given before extensive neurodegeneration has occurred to be effective.

The main target indication for BACE1 inhibitors will likely be for treatment of patients suffering from probable/established AD or those with possible AD dementia. This will be measured by less cognitive and functional decline relative to placebo treatment. There will, however, also be a need to have biomarker data (biochemical and/or neuroimaging) to support an effect on underlying disease pathology. Small molecule inhibitors of BACE1 may have important implications in the treatment of Alzheimer-related dementias. However, despite strong genetic and pharmacological evidence for the involvement of Aβ in the neuropathology of AD, the impact of lowering Aβ on clinical improvement in AD remains to be proven.

Acknowledgments—We thank Kerstin C Nilsson for statistical analysis, Anna Aagaard for crystallization of BACE1, Kristina Eliason, Daniel Bergström, Ann Staflund, and Anette Stålebring Löwstedt for in vivo support, Carina Stephan for formulation support, Anna Bogstedt, and Paulina Appelkvist for Biomarker analysis, Martin Lewin, William Nelson, Kia Strömberg, and Lena Appelsved for in vitro support, Marie Dahlgren for plasma protein binding, Hongmei Yan for Fu brain, and Jessie Dahlström and Yodit Mebratu for bioanalysis.

REFERENCES

1. McKhann, G., Drachman, D., and Folstein, M. (1984) Clinical diagnosis of Alzheimer's disease. Report of the NINCDS-ADRDA work group under the auspices of Department of Health and Human Services Task Force on Alzheimer's disease. *Neurology* **34,** 939–944
2. Querfurth, H. W., and LaFerla, F. M. (2010) Alzheimer's Disease. *N. Engl. J. Med.* **362,** 329–344
3. Alzheimer's Association (2011) 2011 Alzheimer's disease facts and figures. *Alzheimers Dement.* **7,** 208–244
4. Cummings, J. L. (2004) Alzheimer's disease. *N. Engl. J. Med.* **351,** 56–67
5. Ballard, C., Gauthier, S., Corbett, A., Brayne, C., Aarsland, D., and Jones, E. (2011) Alzheimer's disease. *Lancet* **377,** 1019–1031
6. Citron M. (2010) Alzheimer's disease. Strategies for disease modification. *Nat. Rev. Drug Discov.* **9,** 387–398
7. Younkin, S. G. (1995) Evidence that Aβ42 is the real culprit in Alzheimer's disease. *Ann. Neurol.* **37,** 287–288
8. Selkoe, D. J., Yamazaki, T., Citron, M., Podlisny, M. B., Koo, E. H., Teplow, D. B., and Haass, C. (1996) The role of APP processing and trafficking pathways in the formation of amyloid β-protein. *Ann. N.Y. Acad. Sci.* **777,** 57–64
9. Hussain, I., Powell, D., Howlett, D. R., Tew, D. G., Meek, T. D., Chapman, C., Gloger, I. S., Murphy, K. E., Southan, C. D., Ryan, D. M., Smith, T. S., Simmons, D. L., Walsh, F. S., Dingwall, C., and Christie, G. (1999) Identification of a novel aspartic protease (Asp-2) as β-secretase. *Mol. Cell. Neurosci.* **14,** 419–427
10. Sinha, S., Anderson, J. P., Barbour, R., Basi, G. S., Caccavello, R., Davis, D., Doan, M., Dovey, H. F., Frigon, N., Hong, J., Jacobson-Croak, K., Jewett, N., Keim, P., Knops, J., Lieberburg, I., Power, M., Tan, H., Tatsuno, G.,

Tung, J., Schenk, D., Seubert, P., Suomensaari, S. M., Wang, S., Walker, D., Zhao, J., McConlogue, L., and John, V. (1999) Purification and cloning of amyloid precursor protein β-secretase from human brain. *Nature* **402,** 537–540

11. Vassar, R., Bennett, B. D., Babu-Khan, S., Kahn, S., Mendiaz, E. A., Denis, P., Teplow, D. B., Ross, S., Amarante, P., Loeloff, R., Luo, Y., Fisher, S., Fuller, J., Edenson, S., Lile, J., Jarosinski, M. A., Biere, A. L., Curran, E., Burgess, T., Louis, J. C., Collins, F., Treanor, J., Rogers, G., and Citron, M. (1999) β-Secretase cleavage of Alzheimer's amyloid precursor protein by the transmembrane aspartic protease BACE. *Science* **286,** 735–741
12. Yan, R., Bienkowski, M. J., Shuck, M. E., Miao, H., Tory, M. C., Pauley, A. M., Brashier, J. R., Stratman, N. C., Mathews, W. R., Buhl, A. E., Carter, D. B., Tomasselli, A. G., Parodi, L. A., Heinrikson, R. L., and Gurney, M. E. (1999) Membrane-anchored aspartyl protease with Alzheimer's disease β-secretase activity. *Nature* **402,** 533–537
13. Lin, X., Koelsch, G., Wu, S., Downs, D., Dashti, A., and Tang, J. (2000) Human aspartic protease memapsin 2 cleaves the β-secretase site of β-amyloid precursor protein. *Proc. Natl. Acad. Sci. U.S.A.* **97,** 1456–1460
14. Hardy, J., and Selkoe, D. J. (2002) The amyloid hypothesis of Alzheimer's disease. Progress and problems on the road to therapeutics. *Science* **297,** 353–356
15. Hardy, J., and Allsop, D. (1991) Amyloid deposition as the central event in the aetiology of Alzheimer's disease. *Trends Pharmacol. Sci.* **12,** 383–388
16. Lee, V. M., Goedert, M., and Trojanowski, J. Q. (2001) Neurodegenerative tauopathies. *Annu. Rev. Neurosci.* **24,** 1121–1159
17. De Strooper, B., Vassar, R., and Golde, T. (2010) The secretases. Enzymes with therapeutic potential in Alzheimer disease. *Nat. Rev. Neurol.* **6,** 99–107
18. Bateman, R. J., Siemers, E. R., Mawuenyega, K. G., Wen G., Browning K. R., Sigurdson W. C., Yarasheski K. E., Friedrich S. W., Demattos R. B., May P. C., Paul S. M., and Holtzman D. M. (2009) A γ-secretase inhibitor decreases amyloid-β production in the central nervous system. *Ann. Neurol.* **66,** 48–54
19. Holsinger, R. M., McLean, C. A., Beyreuther, K., Masters, C. L., and Evin, G. (2002) Increased expression of the amyloid precursor β-secretase in Alzheimer's disease. *Ann. Neurol.* **51,** 783–786
20. Fukumoto, H., Cheung, B. S., Hyman, B. T., and Irizarry, M. C. (2002) β-Secretase protein and activity are increased in the neocortex in Alzheimer's disease. *Arch. Neurol.* **59,** 1381–1389
21. Zhong, Z., Ewers, M., Teipel, S., Bürger, K., Wallin, A., Blennow, K., He, P., McAllister, C., Hampel, H., and Shen, Y. (2007) Levels of β-secretase (BACE1) in cerebral spinal fluid as a predictor of risk in mild cognitive impairment. *Arch. Gen. Psychiatry* **64,** 718–726
22. Jonsson, T., Atwal, J. K., Steinberg, S., Snaedal, J., Jonsson, P. V., Bjornsson, S., Stefansson, H., Sulem, P., Gudbjartsson, D., Maloney, J., Hoyte, K., Gustafson, A., Liu, Y., Lu, Y., Bhangale, T., Graham, R. R., Huttenlocher, J., Bjornsdottir, G., Andreassen, O. A., Jönsson, E. G., Palotie, A., Behrens, T. W., Magnusson, O. T., Kong, A., Thorsteinsdottir, U., Watts, R. J., and Stefansson, K. (2012) A mutation in APP protects against Alzheimer's disease and age-related cognitive decline. *Nature* **488,** 96–99
23. Singer, O., Marr, R. A., Rockenstein, E., Crews, L., Coufal, N. G., Gage, F. H., Verma, I. M., and Masliah, E. (2005) Targeting BACE1 with siRNAs ameliorates Alzheimer disease neuropathology in a transgenic model. *Nat. Neurosci.* **8,** 1343-1349
24. Stachel, S. J., Coburn, C. A., Sankaranarayanan, S., Price, E. A., Wu, G., Crouthamel, M., Pietrak, B. L., Huang, Q., Lineberger, J., Espeseth, A. S., Jin, L., Ellis, J., Holloway, M. K., Munshi, S., Allison, T., Hazuda, D., Simon, A. J., Graham, S. L., and Vacca, J. P. (2006) Macrocyclic inhibitors of β-secretase. Functional activity in an animal model. *J. Med. Chem.* **49,** 6147–6150
25. McConlogue, L., Buttini, M., Anderson, J. P., Brigham, E. F., Chen, K. S., Freedman, S. B., Games, D., Johnson-Wood, K., Lee, M., Zeller, M., Liu, W., Motter, R., and Sinha, S. (2007) Partial reduction of BACE1 has dramatic effects on Alzheimer plaque and synaptic pathology in APP transgenic mice. *J. Biol. Chem.* **282,** 26326–26334
26. Stanton, M. G., Stauffer, S. R., Gregro, A. R., Steinbeiser, M., Nantermet, P., Sankaranarayanan, S., Price, E. A., Wu, G., Crouthamel, M. C., Ellis, J., Lai, M. T., Espeseth, A. S., Shi, X. P., Jin, L., Colussi, D., Pietrak, B., Huang, Q., Xu, M., Simon, A. J., Graham, S. L., Vacca, J. P., and Selnick, H. (2007) Discovery of isonicotinamide-derived β-secretase inhibitors. *In vivo* reduction of β-amyloid. *J. Med. Chem.* **50,** 3431–3433
27. Stachel, S. J. (2009) Progress toward the development of a viable BACE-1 inhibitor. *Drug Dev. Res.* **70,** 101–110
28. Chang, W. P., Huang, X., Downs, D., Cirrito, J. R., Koelsch, G., Holtzman, D. M., Ghosh, A. K., and Tang, J. (2011) β-Secretase inhibitor GRL-8234 rescues age-related cognitive decline in APP transgenic mice. *FASEB J.* **25,** 775–784
29. Evin, G., Barakat, A., and Masters, C. L. (2010) BACE. Therapeutic target and potential biomarker for Alzheimer's disease. *Int. J. Biochem. Cell Biol.* **42,** 1923–1926
30. May, P. C., Dean, R. A., Lowe, S. L., Martenyi, F., Sheehan, S. M., Boggs, L. N., Monk, S. A., Mathes, B. M., Mergott, D. J., Watson, B. M., Stout, S. L., Timm, D. E., Smith Labell, E., Gonzales, C. R., Nakano, M., Jhee, S. S., Yen, M., Ereshefsky, L., Lindstrom, T. D., Calligaro, D. O., Cocke, P. J., Greg Hall, D., Friedrich, S., Citron, M., and Audia, J. E. (2011) Robust central reduction of amyloid-β in humans with an orally available, non-peptidic β-secretase inhibitor. *J. Neurosci.* **31,** 16507–16516
31. Probst, G., and Xu, Y. Z. (2012) Small-molecule BACE1 inhibitors. A patent literature review (2006–2011). *Expert Opin. Ther. Pat.* **22,** 511–540
32. Xu, Y., Li, M. J., Greenblatt, H., Chen, W., Paz, A., Dym, O., Peleg, Y., Chen, T., Shen, X., He, J., Jiang, H., Silman, I., and Sussman, J. L. (2012) Flexibility of the flap in the active site of BACE1 as revealed by crystal structures and molecular dynamics simulations. *Acta Crystallogr. D. Biol. Crystallogr.* **68,** 13–25
33. Rajendran, L., Schneider, A., Schlechtingen, G., Weidlich, S., Ries, J., Braxmeier, T., Schwille, P., Schulz, J. B., Schroeder, C., Simons, M., Jennings, G., Knölker, H. J., and Simons, K. (2008) Efficient inhibition of the Alzheimer's disease β-secretase by membrane targeting. *Science* **320,** 520–523
34. Sankaranarayanan, S., Holahan, M. A., Colussi, D., Crouthamel, M. C., Devanarayan, V., Ellis, J., Espeseth, A., Gates, A. T., Graham, S. L., Gregro, A. R., Hazuda, D., Hochman, J. H., Holloway, K., Jin L., Kahana, J., Lai, M. T., Lineberger, J., McGaughey, G., Moore, K. P., Nantermet, P., Pietrak, B., Price E. A., Rajapakse, H., Stauffer, S., Steinbeiser, M. A., Seabrook, G., Selnick, H. G., Shi, X. P., Stanton, M. G., Swestock, J., Tugusheva, K., Tyler, K. X., Vacca, J. P., Wong, J., Wu, G., Xu, M., Cook, J. J., and Simon, A. J. (2009) First demonstration of cerebrospinal fluid and plasma Aβ lowering with oral administration of a β-site amyloid precursor protein-cleaving enzyme 1 Inhibitor in nonhuman primates. *J. Pharmacol. Exp. Ther.* **328,** 131–140
35. Malamas, M. S., Robichaud, A., Erdei, J., Quagliato, D., Solvibile, W., Zhou, P., Morris, K., Turner, J., Wagner, E., Fan, K., Olland, A., Jacobsen, S., Reinhart, P., Riddell, D., and Pangalos, M. (2010) Design and synthesis of aminohydantoins as potent and selective human β-secretase (BACE1) inhibitors with enhanced brain permeability. *Bioorg Med Chem Lett* **20,** 6597–6605
36. Patel, S., Vuillard, L., Cleasby, A., Murray, C. W., and Yon, J. (2004) Apo and inhibitor complex structures of BACE (β-secretase). *J. Mol. Biol.* **343,** 407–416
37. Swahn, B. M., Holenz, J., Kihlström, J., Kolmodin, K., Lindström, J., Plobeck, N., Rotticci, D., Sehgelmeble, F., Sundström, M., Berg, S. v., Fälting, J., Georgievska, B., Gustavsson, S., Neelissen, J., Ek, M., Olsson, L. L., and Berg, S. (2012) Aminoimidazoles as BACE-1 inhibitors. The challenge to achieve *in vivo* brain efficacy. *Bioorg. Med. Chem. Lett.* **22,** 1854–1859
38. Leslie, A. G. (1992) *Joint CCP4 + ESF-EAMCB Newsletter on Protein Crystallography* **26,** 27
39. Collaborative Computational Project, Number 4 (1994) The CCP4 suite. Programs for protein crystallography. *Acta Crystallogr. D. Biol. Crystallogr.* **50,** 760–763
40. Murshudov, G. N., Vagin, A. A., and Dodson, E. J. (1997) Refinement of macromolecular structures by the maximum-likelihood method. *Acta Crystallogr. D. Biol. Crystallogr.* **53,** 240–255
41. Bricogne, G., Blanc, E., Brandl, M., Flensburg, C., Keller, P., Paciorek, W., Roversi, P., Sharff, A., Smart, O., Vonrhein, C., and Womack, T. (2010) *AUTOBUSTER*. Global Phasing Ltd, Cambridge, UK
42. Emsley, P., and Cowtan, K. (2004) Coot. Model-building tools for molec-

ular graphics. *Acta Crystallogr. D. Biol. Crystallogr.* **60,** 2126–2132
43. Borgegard, T., Juréus, A., Olsson, F., Rosqvist, S., Sabirsh, A., Rotticci, D., Paulsen, K., Klintenberg, R., Yan, H., Waldman, M., Stromberg, K., Nord, J., Johansson, J., Regner, A., Parpal, S., Malinowsky, D., Radesater, A. C., Li, T., Singh, R., Eriksson, H., and Lundkvist, J. (2012) First and second generation γ-secretase modulators (GSMs) modulate amyloid-β (Aβ) peptide production through different mechanisms. *Alzheimer's Dis. Res. J.* **3,** 29–45
44. Fridén, M., Ducrozet, F., Middleton, B., Antonsson, M., Bredberg, U., and Hammarlund-Udenaes, M. (2009) Development of a high-throughput brain slice method for studying drug distribution in the central nervous system. *Drug Metab. Dispos.* **37,** 1226–1233
45. Di, L., Umland, J. P., Chang, G., Huang, Y., Lin, Z., Scott, D. O., Troutman, M. D., and Liston, T. E. (2011) Species independence in brain tissue binding using brain homogenates. *Drug Metab. Dispos.* **39,** 1270–1277
46. Dayneka, N. L., Garg, V., Jusko, W. J. (1993) Comparison of four basic models of indirect pharmacodynamic responses. *J. Pharmacokinet. Biopharmacol.* **2,** 457–478
47. Post, T. M., Freijer, J. I., Ploeger, B. A., and Danhof, M. (2008) Extensions to the visual predictive check to facilitate model performance evaluation. *J. Pharmacokinet. Pharmacodyn.* **35,** 185–202
48. Geschwindner, S., Olsson, L. L., Albert, J. S., Deinum, J., Edwards, P. D., de Beer, T., and Folmer, R. H. (2007) Discovery of a novel warhead against β-secretase through fragment-based lead generation. *J. Med. Chem.* **50,** 5903–5911
49. Edwards, P. D., Albert, J. S., Sylvester, M., Aharony, D., Andisik, D., Callaghan, O., Campbell, J. B., Carr, R. A., Chessari, G., Congreve, M., Frederickson, M., Folmer, R. H., Geschwindner, S., Koether, G., Kolmodin, K., Krumrine, J., Mauger, R. C., Murray, C. W., Olsson, L. L., Patel, S., Spear, N., and Tian, G. (2007) Application of fragment-based lead generation to the discovery of novel, cyclic amidine β-secretase inhibitors with nanomolar potency, cellular activity, and high ligand efficiency. *J. Med. Chem.* **50,** 5912–5925
50. Albert, J., Arnold, J., Chessari, G., Congreve, M. S., Edwards, P., Murray, C., and Patel, S. (May 24, 2007) PCT International Application WO2007058601
51. Cumming, J. N., Smith, E. M., Wang, L., Misiaszek, J., Durkin, J., Pan, J., Iserloh, U., Wu, Y., Zhu, Z., Strickland, C., Voigt, J., Chen, X., Kennedy, M. E., Kuvelkar, R., Hyde, L. A., Cox, K., Favreau, L., Czarniecki, M. F., Greenlee, W. J., McKittrick, B. A., Parker, E. M., and Stamford, A. W. (2012) Structure based design of iminohydantoin BACE1 inhibitors. Identification of an orally available, centrally active BACE1 inhibitor. *Bioorg. Med. Chem. Lett.* **22,** 2444–2449
52. Arnold, J., Berg, S., Chessari, G., Congreve, M., Edwards, P., Holenz, J., Kers, A., Kolmodin, K., Murray, C., Patel, S., Rakos, L., Rotticci, D., Sylvester, M., and Öhberg, L. (December 27, 2007) Substituted isoindoles as BACE inhibitors and their preparation, pharmaceutical compositions, and use in the treatment of cognitive impairment, Alzheimers disease, neurodegeneration, and dementia PCT International Application WO2007149033
53. Holenz, J., Karlstroem, S., Kolmodin, K., Lindstroem, J., Rakos, L., Rotticci, D., Soederman, P., Swahn, B.-M., and Von Berg, S. (May 20, 2010) Preparation of isoindole derivatives for treatment of amyloid-β protein-related pathologies PCT International Application WO 010056196
54. Swahn, B. M., Kolmodin, K., Karlström, S., von Berg, S., Söderman, P., Holenz, J., Berg, S., Lindström, J., Sundström, M., Turek, D., Kihlström, J., Slivo, C., Andersson, L., Pyring, D., Rotticci, D., Öhberg, L., Kers, A., Bogar, K., Bergh, M., Olsson, L., Janson, J., Eketjäll, S., Georgievska, B., Jeppsson, F., Fälting, J. (2012) Design and synthesis of β-site amyloid precursor protein cleaving enzyme (BACE1) inhibitors with *in vivo* brain reduction of β-amyloid peptides. *J. Med. Chem.*, DOI: 10.1021/jm3009025
55. Janson, J., Eketjäll, S., Yan, H., Tunblad, K., Jeppsson, F., Briem, S., Dahlqvist, C., Radesäter, A. C., Fälting, J., and Visser, S. A. G. (2012) PAGE. Population PKPD modeling of BACE1 inhibitors induced reduction in brain Aβ levels *in vivo*. p. 21
56. Lu, Y., Zhang, L., Nolan, C. E., Becker, S. L., Atchison, K., Robshaw, A. E., Pustilnik, L. R., Osgood, S. M., Miller, E. H., Stepan, A. F., Subramanyam, C., Efremov, I., and Hallgren, A. J., Riddell, D. (2011) Quantitative pharmacokinetic/pharmacodynamic analyses suggest that the 129/SVE mouse is a suitable preclinical pharmacology model for identifying small-molecule γ-secretase inhibitors. *J. Pharmacol. Exp. Ther.* **339,** 922–934
57. Anderson, J. J., Holtz, G., Baskin, P. P., Turner, M., Rowe, B., Wang B., Kounnas, M. Z., Lamb, B. T., Barten, D., Felsenstein, K., McDonald, I., Srinivasan, K., Munoz, B., and Wagner, S. L. (2005) Reductions in β-amyloid concentrations *in vivo* by the γ-secretase inhibitors BMS-289948 and BMS-299897. *Biochem. Pharmacol.* **69,** 689–698
58. Lanz, T. A., Karmilowicz, M. J., Wood, K. M., Pozdnyakov, N., Du P., Piotrowski, M. A., Brown, T. M., Nolan, C. E., Richter, K. E., Finley, J. E., Fei, Q., Ebbinghaus, C. F., Chen, Y. L., Spracklin, D. K., Tate, B., Geoghegan, K. F., Lau, L. F., Auperin, D. D., and Schachter, J. B. (2006) Concentration-dependent modulation of amyloid-β *in vivo* and *in vitro* using the γ-secretase inhibitor, LY-450139. *J. Pharmacol. Exp. Ther.* **319,** 924–933
59. Syvänen, S., Lindhe, O., Palner, M., Kornum, B. R., Rahman, O., Långström, B., Knudsen, G. M., and Hammarlund-Udenaes, M. (2009) Species differences in blodd brain transport of three positron emission tomography radioligands with emphasis on p-glycoprotein transport. *Drug Metab. Dispos.* **37,** 635–643
60. Ito, K., Uchida, Y., Ohtsuki, S., Aizawa, S., Kawakami, H., Katsukura, Y., Kamiie, J., and Terasaki, T. (2011) Quantitative membrane protein expression at the blood-brain barrier of adult and younger cynomolgus monkeys. *J. Pharm. Sci.* **100,** 3939–3950
61. Lu, Y., Riddell, D., Hajos-Korcsok, E., Bales, K., Wood, K. M., Nolan, C. E., Robshaw, A. E., Zhang, L., Leung, L., Becker, S. L., Tseng, E., Barricklow, J., Miller, E. H., Osgood, S., O'Neill, B. T., Brodney, M. A., Johnson, D. S., and Pettersson, M. (2012) CSF Aβ As an effect biomarker for brain Aβ lowering verified by quantitative preclinical analyses. *J. Pharmacol. Exp. Ther.* **342,** 366–375
62. Tai, L. M., Jacobsen, H., Ozmen, L., Flohr, A., Jakob-Roetne, R., Caruso, A., and Grimm, H. P. (2012) The dynamics of Aβ distribution after γ-secretase inhibitor treatment, as determined by experimental and modelling approaches in a wild type rat. *J Pharmacokinet. Pharmacodyn.* **39,** 227–237
63. Lanz, T. A., Wood, K. M., Richter, K. E., Nolan, C. E., Becker, S. L., Pozdnyakov, N., Martin, B. A., Du, P., Oborski, C. E., Wood, D. E., Brown, T. M., Finley, J. E., Sokolowski, S. A., Hicks, C. D., and Coffman, K. J., Geoghegan, K. F., Brodney, M. A., Liston, D., and Tate, B. (2010) Pharmacodynamics and pharmacokinetics of the γ-secretase inhibitor PF-3084014. *J. Pharmacol. Exp. Ther.* **334,** 269–277
64. Beckett, L. A., Harvey, D. J., Gamst, A., Donohue, M., Kornak, J., Zhang, H., and Kuo, J. H. (2010) The Alzheimer's disease neuroimaging initiative. Annual changes in biomarkers and clinical outcomes. *Alzheimers Dement.* **6,** 257–264
65. Das, R., Nachbar, R. B., Edelstein-Keshet, L., Saltzman, J. S., Wiener, M. C., Bagchi, A., Bailey, J., Coombs, D., Simon, A. J., Hargreaves, R. J., and Cook, J. J. (2011) Modeling effect of a γ-secretase inhibitor on amyloid-β dynamics reveals significant role of an amyloid clearance mechanism. *Bull. Math Biol.* **73,** 230–247
66. Visser, S. A. G., Dahlqvist, C., Parkinson, J., Van Schaick, E., Olsson, F., and Lundquist, J. (2012) Abstracts of the Annual Meeting of the Population Approach Group in Europe. ISSN 1871–6032, Abstract 2495, p. 21
67. Braak H., and Braak, E. (1991) Neuropathological staging of Alzheimer-related changes. *Acta Neuropathologica* **82,** 239–259
68. Delano, W. L. (2002) *The PyMOL Molecular Graphis System*, Delano Scientific, Palo Alto, CA
69. Laskowski, R. A., MacArthur, M. W., Moss, D. S., and Thornton, J. M. (1993) *PROCHECK*. A program to check the stereochemical quality of protein structures. *J. Appl. Crystsllogr.* **26,** 283–291